# Optimizing Aircraft Fleet Assignment in Airline Route Networks Using a GA-Based Allocation with Greedy Chain Assignment under Operational Constraints

Huy Van Chau[1], The Hoang Nguyen [2]*, Vo Phi Son[2] and Nguyen The Son[3]

[1]Burnaby South Secondary School, Canada

[2]Vietnam Aviation Academy, Vietnam

[3]University of British Columbia, School of Engineering, Canada

*Corresponding Author/Email: hoangnt@vaa.edu.vn

Manuscript received: December 21, 2025 / Revised: January 30, 2026 / Accepted: March 10, 2026

## ABSTRACT

The fleet assignment problem remains a critical challenge in airline operations, where heterogeneous aircraft must be allocated to scheduled flights in a manner that minimizes total costs while satisfying operational constraints. This paper formulates the problem as a cost minimization model that incorporates both operating expenses and passenger spill costs under constraints of fleet size, airport balance, and time-space network feasibility. Due to the combinatorial nature of the problem, traditional method often faced with poor scalability when increase problem size. To address this, we propose a Genetic Algorithm (GA)-based approach enhanced with a greedy chain assignment and repa ir mechanism to efficiently enforce airport balance and availability constraints. Numerical evaluations are conducted on small-scale and large-scale test cases under multiple cost-per-available-seat-mile (CASM) scenarios. The numerical evaluation highlights the effectiveness and adaptability of the proposed GA-based framework in solving fleet assignment problems.

**KEYWORDS**: Fleet Assignment; Genetic Algorithm; Greedy Chain, Hopcroft-Karp, Cost Optimization

## 1. Introduction

Recently, the aviation industry has experienced increasing pressure to improve operational efficiency and reduce costs while maintaining high levels of service reliability. Rising fuel prices, changing passenger demand, environmental regulations, or intense competition have made efficient resource use a strategic requirement for every airline. Within this context, the airline Fleet Assignment Problem (FAP) plays a crucial role as it determines how different aircraft types are assigned to scheduled flight legs within a given network. The objective is to minimize total cost, which includes explicit operating costs (such as fuel, maintenance, and crew) as well as implicit costs arising from passenger spill when demand exceeds available seat capacity. At the same time, the problem must satisfy a wide range satisfying complex operational constraints, ranging from aircraft balance, airport continuity, and fleet size limitations. These interdependent requirements together make FAP a crucial and complex stage of airline planning.

From a computational standpoint, the FAP is widely recognized as an NP-hard combinatorial optimization problem with complexity escalating significantly with the quantity of flights, aircraft types, and constraints expands. Even moderately sized airline networks can produce problem instances with thousands of binary decision variables with tightly coupled constraints, making exact optimization extremely challenging. According to (Ozdemir et al., 2012), for instance, even with sophisticated commercial solvers, calculating a daily FAP for a medium-sized airline remained challenging, especially when realistic operational constraints are taken into account. Similarly, (Sherali et al., 2006) provide a comprehensive survey of FAP formulations and solution methods, emphasizing that in order to stay tractable at scale, traditional linear and integer programming approaches required relaxation, decomposition, or approximation techniques.

### *1.1. Related Works*

Various approaches have been developed to solve the FAP problem efficiently, ranging from rigorous global optimization to heuristic and metaheuristic solutions; each aiming to increase the complexity and practicality of the problem. Classical Integer Linear Programming (ILP) and Mixed-Integer Linear Programming (MILP) models were the traditional approach and form the theoretical foundation of FAP research. They reach globally optimal solutions using rigorous mathematical foundation under deterministic assumptions and well-defined constraints (Abara, 1989). Afterwards, extensions using network-flow and flight-string formulations further improved modeling fidelity by explicitly enforcing aircraft balance and rotation feasibility (Hane et al., 1995). However, despite these advances, exact methods remain computationally burdensome, especially for large-scale airline networks.

To overcome these challenges, metaheuristic algorithms

have been introduced as alternative solutions. Among these, the Ant Colony Optimization (ACO) algorithm has demonstrated promising results for complex optimization problems. Specifically, (Rashid Anzoom and Ahsan, 2018) applied ACO to the FAP, showing that this approach can effectively identify near-optimal fleet assignments with improved convergence speed. However, while ACO performs well for small and medium-scale problems, its convergence quality tends to deteriorate when the problem dimension increases, and it often requires extensive parameter tuning for consistent results. In addition, Genetic Algorithm (GA)-based techniques have gained popularity due to their adaptability and ability to handle nonlinear optimization problems. Although this hybrid approach offers flexibility and good convergence, it easily violates operational constraints during evolution, leading to infeasible solutions (Okafor et al., 2019). Similarly, (Li and Tan, 2013) treated the FAP as an unconstrained intelligent optimization problem by embedding constraints into the fitness function. While this formulation simplifies the GA structure, it increases the risk of never reaching a feasible yet satisfactory solution, as constraint satisfaction becomes a secondary optimization objective.

### *1.2. Motivations And Contributions*

***Motivation:*** Motivated by the limitations of existing methods, this paper proposes a constraint-aware Genetic Algorithm framework for solving the fleet assignment problem efficiently and feasibly. The proposed approach integrates a Greedy Chain Assignment and a repair mechanism within the GA framework. The Greedy Chain Assignment ensures that each chromosome maintains operational feasibility by constructing valid aircraft rotation chains that respect flight connectivity and airport balance. The repair mechanism subsequently adjusts infeasible solutions by reassigning aircraft types to flights, ensuring compliance with fleet-size and continuity constraints. As a result, the proposed method not only maintains the exploration and global search strengths of the GA but also effectively prevents constraint violations commonly observed in traditional heuristic methods.

***Contributions:*** In this study, we formulate the fleet assignment problem as a mixed-integer cost minimization model that integrates both operating and spill cost components under stochastic passenger demand. Unlike established GA-based approaches that rely heavily on penalty functions to handle infeasible solutions, the proposed method introduces a chain-based solution representation in which feasible aircraft rotation chains are first constructed from the flight compatibility network using the Hopcroft–Karp maximum matching algorithm. These chains are then assigned aircraft types through a greedy chain assignment mechanism that minimizes incremental cost while respecting fleet availability. In addition, a repair procedure integrated within the GA evolution process is used to enforce airport balance and fleet-size constraints, improving feasibility throughout the search process. By combining graph-based preprocessing with evolutionary optimization, the proposed approach significantly reduces the generation of infeasible solutions and improves convergence stability, enabling efficient near-optimal solutions for both small-scale and large-scale fleet assignment instances. Our approach is tested on small- and large-scale flight networks to demonstrate scalability and robustness. Numerical results show that the proposed GA-based model converges to near-optimal solutions with significantly reduced computation time compared to conventional methods while ensuring full feasibility under all operational constraints.

The rest of this paper is organized as follows. Section II introduces the system description and formulates the problem mathematically. Section III presents the proposed GA-based allocation model with the Greedy Chain Assignment and repair mechanism. Section IV discusses the simulation setup and evaluates the numerical results for a small-scale instance to verify its validity, while Section V uses a large-scale instance to assess its computational performance. Finally, Section VI concludes the paper and outlines future research directions.

## 2. System Description And Problem Formulation

### *2.1. System Description*

The problem formulated as assigning a heterogenous fleet of aircraft types $\mathrm{j} \in K$ to a set of scheduled flights $\mathrm{i} \in F$ which objective is minimizing total operating cost while maintaining oprational and balance constrains. Each flight i is defined by its origin $o_i$, destination $d_i$, scheduled departure time $t_i^{dep}$, scheduled arrival time $t_i^{arr}$, mean passenger demand $\mu_i$, standard deviation of demand $\sigma_i$, and flight distance $\mathrm{Dis}t_i$. Each aircraft type j is characterized by the seat capacity $\mathrm{Sea}t_j$, unit operating cost per available seat-mile $\mathrm{CAS}M_j$, unit revenue per available seat-mile $\mathrm{RAS}M_j$, and the available fleet size $N_j$. For a given flight i and aircraft type j, the total cost is the sum of the operating cost and the spill cost, formulated as

$$c_{i,j} = c_{i,j}^{o} + c_{i,j}^{s} \tag{1}$$

The operating cost $c_{i,j}^{o}$ is computed as

$$c_{i,j}^{o} = \mathrm{CAS}M_j \cdot Seat_j \cdot Dist_i \tag{2}$$

and the spill cost is computed as

$$c_{i,j}^{s} = \mathrm{Ps}_{i,j} \cdot Seat_j \cdot Dist_i \cdot r_{sp} \tag{3}$$

where $r_{sp}$ represents the spill rate or lost rate (%) of passengers to other airlines, and $\mathrm{Ps}_{i,j}$ is is the expected number of passengers spilled when assigning type j to flight i, which is calculated as $\int_c^{\infty}(x-c)f(x)dx$ in which $\mathrm{c} = \mathrm{Sea}t_j$, $\mathrm{f}(x)$ is the probability distribution function of the respective demand $\mu_i$.

*Nomenclature*

$i \in F$ : : Set of scheduled flights, indexed by $i$
$j \in K$ : Set of aircraft types, indexed by $j$
$m \in M$ : Set of nodes in the time-space network
$Seat_j$ : Seat capacity of aircraft type $j$
$CASM_j$ : Unit operating cost per available seat-mile of aircraft type $j$
$RASM_j$ : Unit revenue per available seat-mile of aircraft type $j$
$N_j$ : Available fleet size of aircraft type $j$
$\mu_i$ : Mean passenger demand of flight $i$
$\sigma_i$ : Standard deviation of passenger demand of

flight $i$

$Dist_i$ : Flight distance of flight $i$

$t_i^{dep}$ : Scheduled departure time of flight $i$

$t_i^{arr}$ : Scheduled arrival time of flight $i$

$o_i$ : Origin airport of flight $i$

$d_i$ : Destination airport of flight $i$

$T_{max}$ : Maximum number of generations in GA

$P$ : Population size

$P^e$ : Elite population size

$Ps_{i,j}$ : Expected number of passengers spilled when assigning type $j$ to flight $i$

$r_{sp}$ : Spill rate or lost passenger rate (%)

$c_{i,j}^s$ : Spill cost of assigning type $j$ to flight $i$

$c_{i,j}^o$ : Operating cost of assigning type $j$ to flight $i$

$c_{i,j}$ : Total cost of assigning type $j$ to flight $i$

### *2.2. Problem formulation*

The objective function is to minimize the total cost of assigning aircraft types to all scheduled flights, formulated as

$$\min\left(Z = \sum_{j\in K}\sum_{i\in F} c_{ij}\ x_{ij}\right) \quad (4)$$

Subject to

$$\sum_{j\in K} x_{ij} = 1 \quad \forall i \in F \quad (5)$$

$$G_{m,j} = G_{m-1,j} + \sum_{i\in F} S_{i,m}\cdot x_{ij}, \quad \forall m \in M,\ \forall j \in K \quad (6)$$

$$\sum_{i:\mathrm{dep}(i)=a} x_{ij} = \sum_{i:\mathrm{arr}(i)=a} x_{ij}, \quad \forall a \in A,\ \forall j \in K \quad (7)$$

$$G_{m,j} \le N_j, \quad \forall m \in M,\ \forall j \in K \quad (8)$$

In. which $x_{i,j}$, representing the decision variable, equals 1 if flight $i$ is assigned to aircraft type $j$, otherwise zero. The objective function (4) minimizes the total assignment cost.

The constraint (5) ensures that each flight is covered by exactly one aircraft type. The condition (6) ensures that an aircraft of the correct type will be available at the right place and the right time, in which $G_{m,j}$ denotes the number of aircraft of fleet type $j$ on the ground at node $m \in M$, where $M$ is the set of nodes in the time-space flight network, and $S_{i,m}$ takes the value $+1$ for arrivals and $-1$ for departures.

The constraint (7) enforces airport balance for each aircraft type over the planning schedule, where the total number of departures from an airport equals the total number of arrivals to that airport for the same fleet type. The constraint (8) reflects the fleet size $N_j$ pertaining to each aircraft type $j$, ensuring that the number of aircraft in use at any node does not exceed the total available.

## 3. Proposed approach

The proposed methodology adopts a Genetic Algorithm (GA) scheme with multiple combinatorial operators to minimize the total cost subject to operational constraints. Given the complexity of the airport balance constraint (7), simple GA approach was insufficient, which require an integration of combination of greedy chain assignment and repair mechanism.

Initially, we employed a maximum generation $T_{max}$ and a population size $P$. Each GA chromosome $N$ represents an allocation matrix $A = [a_{j,m}]$, denoting the number of aircraft type $j$ stationed at airport $m$ at the start of the schedule. This representation inherently satisfies fleet size constraints by ensuring that $\sum_m a_{j,m} = N_j$ for each type $j$. An availability vector $A_{j,m}$ is maintained to track the number of unassigned aircraft of type $j$ at airport $m$.

It should be noted that the GA does not directly manipulate the binary decision variables $x_{i,j}$introduced in the MILP formulation. Instead, the algorithm constructs aircraft chains and assigns each chain to a specific aircraft type. Once the assignment process is completed, the corresponding decision variables $x_{i,j}$can be derived directly from the resulting schedule, where $x_{i,j} = 1$ if flight $i$ belongs to a chain operated by aircraft type $j$ and $x_{i,j} = 0$ otherwise. Since each flight appears in exactly one chain and each chain is assigned to a single aircraft type, constraint (5) is naturally satisfied.

The chain assignment procedure begins with a flight connectivity preprocessing step. A directed compatibility graph $G = (V_L, V_R, E)$ is constructed where each flight is represented twice, once as a potential predecessor node (left set) and once as a potential successor node (right set). An edge $(i_x^L, i_y^R) \in E$ is added if flight $y$ can depart from the arrival airport of flight x no earlier than its arrival time. The Hopcroft-Karp algorithm is then applied to this bipartite graph to obtain a maximum matching, which identifies the largest possible set of direct flight-to-flight connections without conflicts. Subsequently, a minimum path cover of the flight set $F$ is derived, where each path corresponds a chain that can be operated by a single aircraft. These initial flight chains $B$ are sorted according to descending number of flights, followed by ascending departure time of the first flight, and then by original index.

For each chain $b \in B$, the algorithm evaluates all feasible aircraft types satisfying $A_{j,m_0} > 0$, where $m_0$ is the departure airport of the chain's first flight. The incremental cost $\Delta Z_{j,b}$ of assigning type $j$ was computed as (1) with $Ps_{i,j}$ estimation by assuming the passenger demand $D_i \sim \mathcal{N}(\mu_i, \sigma_i^2)$. Aircraft type $j^*$ with minimal $\Delta Z_{j,b}$ is selected, $A_{j^*,m_0}$ is decremented, and the chain's terminal airport $m$ is recorded for balance tracking. If there is no feasible type exists, the chromosome is flagged infeasible and penalized.

The GA evolves over generations using selection, crossover, repair, mutation, and elite preservation. At each generation $i$, the top $P^e$ individuals, ranked lexicographically by imbalance and cost $Z$, form the parent pool. Each offspring was produced by inheriting each element $a_{j,m}^{(0)}$, refering to the number of aircraft $j$ assigned to start at airport $m$, from parent $p_1$ if $r_{j,m} < 0.5$, and from parent $p_2$ otherwise, where $r_{j,m} \sim U(0,1)$. However, since each offspring may be created with $\sum_m a_{j,m} = N_j$ unstisfaction, a repair operator $R$ is applied, which excess aircrafts type will either be added or removed until the equality holds, with adjustments made to minimize imbalance and cost. With probability $p_{mut}$, mutation will

occcured, performing a neighbor move $n^a_{j,m'} = n_{j,m'} + 1$, $n^a_{j,m''} = n_{j,m''} - 1$ for randomly selected airports $m', m''$ while preserving capacity constraints.

The algorithm gradually seeks a solution which satisfy constrain (7) while preserving other constrains satisfactory before performing cost optimization. Iterations continue until $T_{max}$ generations are reached, or no improvement is observed, producing a final allocation that satisfies all constraints with minimal cost

**Algorithm 1: GA-based combinatorial Algorithm for FAM**

**Input:** Flight set $F$, aircraft type $j \in J$, fleet size $N_j$ airports $M$, GA parameters $T_{max}, P, P^e, p_{mut}$

Construct compatibility graph $G$ and apply Hopcroft-Karp algorithm to obtain maximum matching

Derive minimum path cover of $F$ from matching to form initial chains $B$

Sort $B$ by: (i) descending number of flights, (ii) ascending first departure time, (iii) original index.

**Initialization:** For $p = 1$ to $P$, generate random $A^p = [A^p_{j,m}]$ satisfying $\sum_m a_{j,m} = N_j$, and assign chains greedily using $\Delta Z^0_{j,b}$

**Evaluate** cost $Z^p$ and imbalance $I^p$ for each chromosome.

**Find initial best population:** $A^g = A^b$ with $I^b = min(I^p), Z^b = min(Z^p)$

**for** $t = \mathbf{1}$ to $T_{max}$ **do**

**Selection:** Select top $P^e$ by lexicographic order (imbalance, $Z$) as parents, discard the rest

**Crossover:** Generate $P_{new} = P - P^e$ population

for each $p_{\text{new}} \in P_{new}$, inherit $a^{(0)}_{j,m}$ from either parents $(p_1, p_2)$, chosen uniformly at random $\forall (j, m)$

**Repair:** for each $j$, adjust $a^{(0)}_{j,m}$ until $\sum_m a_{j,m} = N_j$ with $(I, Z)$ aware

**Mutation:** With probability $p_{mut}$, select $(j, m', m'')$ and update with constrains aware

$$a_{j,m'} \leftarrow a_{j,m'} + 1, \quad a_{j,m''} \leftarrow a_{j,m''} - 1$$

**Greedy-repair:** Assign chains $B$ to $(j, m)$ pairs with minimal $\Delta Z^0_{j,b}$, constrants aware

**Evaluation:** cost $Z^p$ and imbalance for each chromosome

**if** $I^o < I^{gb}$ or $(I^o = I^{gb}$ and $Z^o < Z^{gb})$ **then**

$A^{gb} \leftarrow A^o, B^{gb} = \{b_o \in B\}, \quad Z^{gb} \leftarrow Z^o, \quad I^{gb} \leftarrow I^o,$

e**nd if**

**end for**

**for** each chain $b \in B^{bg}$ assigned to type $j$ **do**

$\forall i \in B, x_{i,j} = 1$ and $x_{i,j'} = 0$ for all $j \neq j'$

**end for**

**Output:** Final allocation $A^{gb}, B^{gb}$, with $I^{gb} = 0$ and minimal $Z^{gb}$

## 4. Small-scaled Cost optimisation Numerical evaluation

In this section, we will examine the proposed algorithm for the problem. First, a small-scaled case with known global minimal cost, respecting all constrains is considered. For spill cost calculation, we assumed the passenger demand follows a normal distribution, $r_{sp} = 85\%$. The selection of this spill rate is predicated on a conservative assumption frequently employed in capacity planning analyses; specifically, a substantial portion of spilled demand is considered lost revenue to underscore the operational expenses associated with inadequate capacity. Similar assumptions have been used in past studies of airline scheduling and spill cost modeling, where fixed spill ratios are used when detailed passenger recapture data are unavailable. However, the exact spill ratio depends on things like how well the network is connected, how easy it is for passengers to be recaptured, and how airlines handle rebooking. Despite this, using a fixed value allows the model to effectively show the economic effects of unmet demand, even without specific data for each route, while also being computationally efficient. Regarding GA, $P^e = \frac{1}{2}P, P_{mute} = 0.2,$ the crossover rate is 0.8. Simulations are conducted bases on changing cost scenarios (CASM 1-5).

### *4.1. Small-scaled Cost optimization simulation setup*

The data pertaining to the airline, comprising a fleet of five aircraft types with their corresponding RASM, seat capacity, and availability, are assumed as shown in Table 1. RASM values are assumed for simulation purposes with reference to (Huang et al., 2021) and seat capacity is taken from Vietnam Airline's seat configeration (Vietnam Airlines, 2019). The CASM for all scenarios is assumed in Table 2. Here, we examine operational daily sub-schedule comprising of 42 separate flight segments.

**Table 1:** Aircraft max number, seat configurations, respective unit costs and unit revenues

| Aircraft type | Aircraft number (max) | Configuration (Seats) | RASM in USD |
|---|---|---|---|
| A320 | 3 | 186 | 0.25 |
| A321 | 41 | 184 | 0.25 |
| A350 | 14 | 305 | 0.30 |
| B787-9 | 11 | 274 | 0.30 |
| B787-10 | 6 | 274 | 0.30 |

**Table 2:** CASM Evolution by Aircraft Type

| Aircraft type | CASM (1) | CASM (2) | CASM (3) | CASM (4) | CASM (5) |
|---|---|---|---|---|---|
| A320 | 0.0912 | 0.0708 ↓ | 0.0997 ↑ | 0.1301 ↑ | 0.1639 ↑ |
| A321 | 0.1158 | 0.0899 ↓ | 0.1266 ↑ | 0.1652 ↑ | 0.2081 ↑ |
| A350 | 0.1031 | 0.0816 ↓ | 0.1120 ↑ | 0.1437 ↑ | 0.1788 ↑ |
| B787-9 | 0.1029 | 0.0819 ↓ | 0.1116 ↑ | 0.1426 ↑ | 0.1765 ↑ |
| B787-10 | 0.0925 | 0.0753 ↓ | 0.0998 ↑ | 0.1250 ↑ | 0.1518 ↑ |

## 4.2. Small-scaled Cost optimisation numerical result

**Table 3:** Optimized Solutions across CASM Scenarios — Flight count and Percentage by Aircraft Type

| | CASM 1 | CASM 2 | CASM 3 | CASM 4 | CASM 5 |
|---|---|---|---|---|---|
| Aircraft | Flights /% | Flight/% | Flight/% | Flight/% | Flight/% |
| A320 | 6/14.29% | 6/14.29% | 6/14.29% | 6/14.29% | 6/14.29% |
| A321 | 34/80.95% | 36/85.71% | 36/85.71% | 32/76.19% | 34/80.95% |
| A350 | 0/0.00% | 00.00% | 00.00% | 00.00% | 0/0.00% |
| B787-9 | 0/0.00% | 0/0.00% | 0/0.00% | 0/0.00% | 0/0.00% |
| B787-10 | 2/4.76% | 0/0.00% | 0/0.00% | 4/9.52% | 2/4.76% |
| Total | 42/100% | 42/100% | 42/100% | 42/100% | 42/100% |

Table 3 illustrates the assigning distribution of different aircraft type. It is observable that the major chosen aircrafts were mostly narrow body type, A321 and A320, which offer adequate capacity characteristic that better matched the assume demand, resulting in lower spill cost. Regarding wide-body aircrafts, even though both B787-9 and B787-10 are necessarily the same except for CASM, which B787-10 were always more affordable. Such different resulted in the exploitation of B787-10 throughout all CASM scenarios while B787-9 were never used.

**Table 4:** Optimized Solutions across CASM Scenarios - Aircraft Count and Percentage by Type

| | CASM 1 | CASM 2 | CASM 3 | CASM 4 | CASM 5 |
|---|---|---|---|---|---|
| Aircraft | Count/% | Count/% | Count/% | Count/% | Count/% |
| A320 | 3/12.00% | 3/11.54% | 3/12.50% | 3/11.54% | 3/12.50% |
| A321 | 20/80.00% | 23/88.46% | 21/87.50% | 20/76.92% | 20/83.33% |
| A350 | 0/0.00% | 0/0.00% | 0/0.00% | 0/0.00% | 0/0.00% |
| B787-9 | 0/0.00% | 0/0.00% | 0/0.00% | 0/0.00% | 0/0.00% |
| B787-10 | 2/8.00% | 0/0.00% | 0/0.00% | 3/11.54% | 1/4.17% |
| Total | 25/100% | 26/100% | 24/100% | 26/100% | 24/100% |

Observably, in Table 4, the fleet remained dominated by the A321, accounting for 76.92-88.46% of aircraft in each scenario, with the A320 maintaining constant (3)and the B787-10 appearing intermittently (0-11.54%), while the A350 and B787-9 were absent operationally. An absent ofB787-10 in scenarios were likely caused by a significant reduced in CASM for narrowbodies, likely resulting in lower spill cost, which can cause the demand distribution less effect. As CASM increased back in scenario 3, yet distribution remained unchanged, indicating reliance on the core narrowbody fleet despite increased costs. The shift in CASM 3 to CASM 4 saw a substantial rise, prompting reintroduction and expansion of B787-10 to 11.54% to offset unit cost escalation on long-haul segments. However, even though between CASM 4 and 5 continued an upward trend, B787-10 share was reduced to 4.17%.

Table 5 depicts the total cost progression and changes in aircraft cost shares and the disparities between the proposed algorithm and the known global best value, gained through linear programming. The A321 consistently contributed the majority of total costs, peaking in CASM 2 in conjunction with its highest fleet share and lowest CASM value, indicating high utilization of this type during cost-efficient phases. The A320 maintained a relatively stable contribution across all scenarios, with absolute costs increasing from 268,349 (CASM 1) to 477,307 (CASM 5), reflecting both CASM. The B787-10 showed intermittent cost participation, mirroring its fluctuating operational role identified in the fleet distribution analysis, with deployments aligning to periods of rising CASM for narrowbodies. No costs were incurred for the A350 or B787-9 in any scenario, consistent with their absence from the operational fleet. Total cost declined from CASM 1 to CASM 2 due to across-the-board CASM reductions, then increased steadily to CASM with the largest absolute gain from CASM 3 to CASM 4 driven primarily by the A321 and the reintroduction of the B787-10. Percentage error against global best cost remained below 0.41% across all scenarios, confirming close model-to-target alignment with only slightly different, while shifts in type-specific cost contributions were driven predominantly by changes in CASM.

**Table 5:** Optimized Solutions across CASM Scenarios - Aircraft Cost and Percentage by Type

| | CASM 1 | CASM 2 | CASM 3 | CASM 4 | CASM 5 |
|---|---|---|---|---|---|
| Aircraft | Cost/% | Cost/% | Cost/% | Cost/% | Cost/% |
| A320 | $268,349/ 25.96% | $216,312/ 26.43% | $297,342/ 26.44% | $384,361/ 26.63% | $477,307/ 26.49% |
| A321 | $709,877/ 68.68% | $602,052/ 73.57% | $827,078/ 73.56% | $932,159/ 64.58% | $1,233,366/ 68.46% |
| A350 | $0/ 0.00% | $0/ 0.00% | $0/ 0.00% | $0/ 0.00% | $0/ 0.00% |
| B787-9 | $0/ 0.00% | $0/ 0.00% | $0/ 0.00% | $0/ 0.00% | $0/ 0.00% |
| B787-10 | $55,416/ 5.36% | $0/ 0.00% | $0/ 0.00% | $126,964/ 8.80% | $90,837/ 5.04% |
| Total | $1,033,641/ 100.00% | $818,364/ 100.00% | $1,124,420/ 100.00% | $1,443,484/ 100.00% | $1,801,510/ 100.00% |
| Global best | $1,030,286 | $815,060 | $1,120,088 | $1,440,406 | $1,795,074 |
| Percentage error | 0.3256 | 0.4054 | 0.3868 | 0.2137 | 0.3585 |

### 4.3 Implementation Details and Verification

The numerical experiments were implemented in Python 3.10, where the proposed GA, Greedy Chain Assignment procedure, and repair mechanisms were developed using standard Python libraries (Math, Random, Copy, Time, Collections, Dataclasses, Datetime). Using NumPy, we performed numerical calculations and modeled demand using a stochastic approach. The flight connectivity graph and the construction of aircraft chains were accomplished through a custom implementation of the Hopcroft-Karp algorithm, which we developed to find the best matches in a bipartite graph. This method allows us to efficiently create valid flight chains within the time-space network before we assign specific aircraft types.

The expected passenger spill was calculated using an analytical formula, derived from the truncated normal distribution. This method provides a direct approximation of the expected spill, assuming passenger demand follows a normal distribution. This approach significantly reduces computational requirements compared to Monte Carlo simulation, while still maintaining numerical accuracy. For validation purposes, the implementation also supports a simulation-based spill estimation using random sampling.

The sensitivity analysis of key GA parameters is illustrated in Figures 1, 2, and 3, where the optimized cost is evaluated across five CASM scenarios. Due to the high stability of the algorithm, there are no significant differences observed across all 5 CASM scenarios when the analysis is conducted using the small-scale 42-flight instance presented in Section 4. Therefore, for clearer visualization and more meaningful analysis, the large-scale 550-flight scenario presented in Section 5 is used instead.

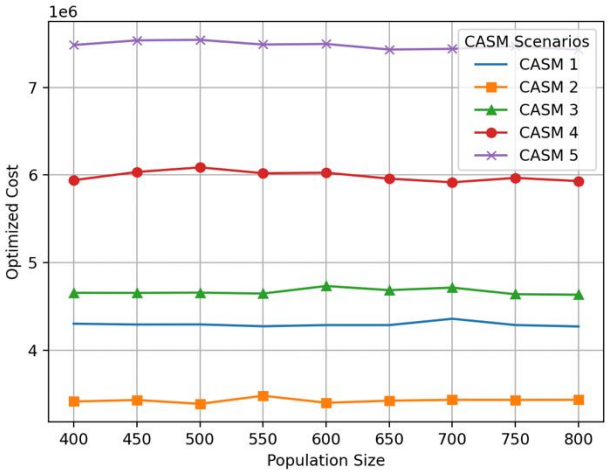


**Figure 1:** Population Size Analysis

From Figure 1, the results remain highly stable over the range of 400 to 800. All CASM scenarios demonstrate only minor variations in overall cost, suggesting the algorithm's insensitivity to population size within this range. Nevertheless, a somewhat greater degree of variability is evident between 550 and 650, potentially due to diminished selection pressure and the augmented computational demands per generation linked to larger populations. This can impede convergence and restrict the algorithm's capacity to efficiently capitalize on superior solutions within a predetermined generation limit. Increasing the population size beyond 500 doesn't significantly improve the results. This suggests that the improvements in solution quality are small compared to the computational resources used.

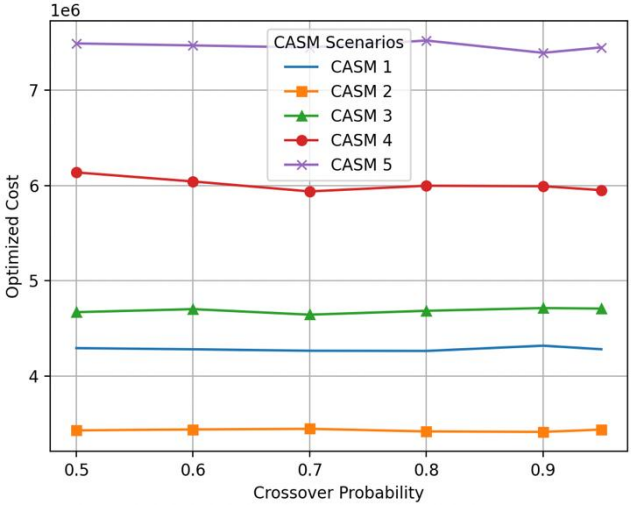


**Figure 2:** Crossover Probability Analysis

Similarly, the data in Figure 2 shows consistent performance across the crossover probability range of 0.5 to 0.95. All CASM scenarios show minimal variation in optimized cost, suggesting that the algorithm is relatively insensitive to crossover probability within this interval. Improvements are

evident within the 0.7-0.85 range for certain scenarios (CASM 1 and CASM 3).

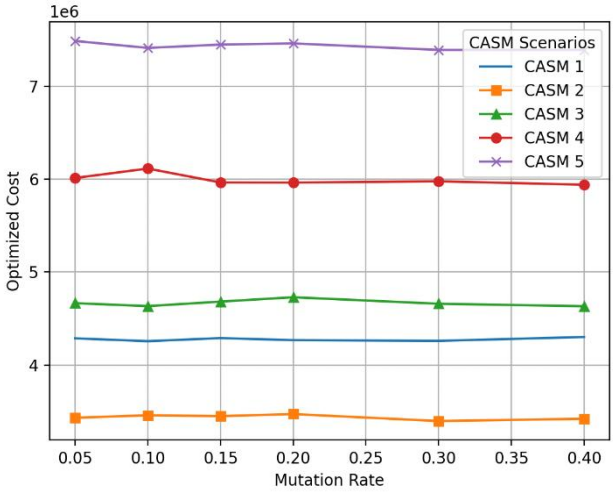


**Figure 3:** Mutation Rate Analysis

Figure 3 further illustrates the impact of crossover probability on solution quality. The findings suggest that altering the crossover probability between 0.05 and 0.4 produces marginal changes in the optimized cost. Slight fluctuations are apparent within the lower mutation rate range (0.05-0.20), potentially due to inadequate population diversity, which restricts the algorithm's capacity to circumvent local optima, thereby yielding somewhat less consistent performance.

Across the evaluated configurations, the key GA parameters (population size, crossover probability, and mutation rate) demonstrated consistent performance. This relative insensitivity to parameter adjustments can be explained by the chain-based solution representation, which, by virtue of its design, ensures feasibility through the pre-optimization construction of valid aircraft rotations. Consequently, the search space navigated by the GA is both significantly reduced and structured, thereby fostering more stable convergence behavior when contrasted with methodologies that utilize direct assignment encoding. The chosen parameter settings for both numerical analysis in Section 4 and 5 (population size = 600, crossover rate = 0.8, mutation rate = 0.2) creates an effective balance between solution quality and computational efficiency.

To verify the correctness of the algorithm, the small-scale test instance was additionally solved using an exact linear programming formulation to obtain the global optimal solution. The solutions produced by the proposed GA-based method were compared with this optimal benchmark. As shown in Table 5, the obtained results remain within 0.21%-0.41% of the global optimum across all CASM scenarios, confirming the correctness and reliability of the implementation.

## 5. Large-scaled Cost optimisation Numerical evaluation

In this section, we will examined the proposed algorithm for the problem and evaluate its scalability. This large-scaled case is respecting all constrains is considered. Simulations are conducted also bases on changing cost scenarios (CASM 1-5). Here, we used the same assumption as the small-scaled one, yet with a different flight number.

### *5.1. Large-scaled Cost optimization Simulation Setup*

We used a schedule comprising 550 flights, operated by the available fleet with their respective characteristics, as presented in Table 6, based on data referenced from (Huang et al., 2021) and (Vietnam Airlines, 2019). We will be examined with practical CASM scenarios for all fleet types, shown in Table 7. The flight network is referenced and built from Vietnam domestic flights schedule.

**Table 6:** Aircraft max number, seat configurations, respective unit costs and unit revenues

| Aircraft | Count (N) | Seats | RASM |
|---|---|---|---|
| A320 | 15 | 186 | 0.25 |
| A321 | 75 | 184 | 0.25 |
| A350 | 8 | 305 | 0.30 |
| B787-9 | 12 | 274 | 0.30 |
| B787-10 | 18 | 274 | 0.30 |
| ATR72 | 17 | 68 | 0.40 |
| E190 | 7 | 100 | 0.35 |
| A319 | 5 | 144 | 0.25 |
| A321neo | 23 | 230 | 0.25 |
| B737-8 | 19 | 178 | 0.25 |

**Table 7:** CASM Evolution by Aircraft Type

| AIRCRAFT | CASM 1 | CASM 2 | CASM 3 | CASM 4 | CASM 5 |
|---|---|---|---|---|---|
| A320 | 0.0912 | 0.0708 ↓ | 0.0997 ↑ | 0.1301 ↑ | 0.1639 ↑ |
| A321 | 0.1158 | 0.0899 ↓ | 0.1266 ↑ | 0.1652 ↑ | 0.2081 ↑ |
| A350 | 0.1031 | 0.0816 ↓ | 0.1120 ↑ | 0.1437 ↑ | 0.1788 ↑ |
| B787-9 | 0.1029 | 0.0819 ↓ | 0.1116 ↑ | 0.1426 ↑ | 0.1765 ↑ |
| B787-10 | 0.0925 | 0.0753 ↓ | 0.0998 ↑ | 0.1250 ↑ | 0.1518 ↑ |
| ATR72 | 0.1784 | 0.1439 ↓ | 0.2013 ↑ | 0.2612 ↑ | 0.3284 ↑ |
| E190 | 0.1362 | 0.1098 ↓ | 0.1502 ↑ | 0.1939 ↑ | 0.2404 ↑ |
| A319 | 0.1211 | 0.0973 ↓ | 0.1331 ↑ | 0.1709 ↑ | 0.2118 ↑ |
| A321neo | 0.1087 | 0.0845 ↓ | 0.1195 ↑ | 0.1561 ↑ | 0.1953 ↑ |
| B737-8 | 0.0982 | 0.0771 ↓ | 0.1069 ↑ | 0.1372 ↑ | 0.1695 ↑ |

### 5.2. Large-scaled Cost optimisation numerical result

Table 8 shows the optimized flight allocation across CASM scenarios. The distribution has a strong preference for narrowbody aircraft, particularly the A321 and B737-8, due to their competitive CASM values (0.0899-0.2081 for the A321 and 0.0771-0.1695 for the B737-8) and adequate seat capacities

for most demand profiles of the network. The A321 consistently led of total flights, supported by its high availability and favorable RASM-to-CASM margin, while the A320 maintained 16.18-21.27% share despite. The B737-8 retained stable at 24-26%, suggesting because of its compatibility and low CASM in the network The B787-10, having a relatively low CASM among widebodies (0.0753-0.1518) and high seating capacity (274 seats), appeared selectively in CASM 2-5, indicating targeted long-haul deployment for high-demand flights when narrowbody CASM increased. Smaller aircraft such as the E190 and A319 gained share toward later scenarios as rising CASM favored capacity rightsizing to avoid revenue dilution, while the A321neo only been used in CASM 2-4.

It is also important to noted why A350, B787-9, and ATR72 consistently record zero allocations in Table 8. The simulated network represents primarily Vietnam domestic routes, which are largely short- to medium-haul with moderate demand levels. Under these conditions, narrowbody aircraft provide a more efficient capacity-to-cost balance. The A350 and B787-9, although capable of carrying large passenger volumes, have seating capacities (305 and 274 seats respectively) that exceed the demand levels of most flights in the network. Deploying these aircraft would therefore increase operating costs without generating proportional revenue, making them economically unattractive for the optimization objective. Similarly, the ATR72, despite its suitability for short-haul operations, exhibits the highest CASM among the tested aircraft types, and its smaller seating capacity (68 seats) results in higher effective cost per transported passenger compared with alternatives such as the E190 or A319. Consequently, the optimization algorithm consistently excludes these aircraft types from the optimal solution.

**Table 8:** Optimized Solutions across CASM Scenarios — Flight count and Percentage by Aircraft Type

| | CASM 1 | CASM 2 | CASM 3 | CASM 4 | CASM 5 |
|---|---|---|---|---|---|
| AIRCRAFT | Flights/% | Flights/% | Flights/% | Flights/% | Flights/% |
| A320 | 108/ 19.64% | 117/ 21.27% | 114/ 20.73% | 89/ 16.18% | 108/ 19.64% |
| A321 | 275/ 50.00% | 242/ 44.00% | 235/ 42.73% | 241/ 43.82% | 228/ 41.45% |
| A350 | 0/ 0.00% | 0/ 0.00% | 0/ 0.00% | 0/ 0.00% | 0/ 0.00% |
| B787-9 | 0/ 0.00% | 0/ 0.00% | 0/ 0.00% | 0/ 0.00% | 0/ 0.00% |
| B787-10 | 0/ 0.00% | 19/ 3.45% | 12/ 2.18% | 15/ 2.73% | 13/ 2.36% |
| ATR72 | 0/ 0.00% | 0/ 0.00% | 0/ 0.00% | 0/ 0.00% | 0/ 0.00% |
| E190 | 3/ 0.55% | 0/ 0.00% | 5/ 0.91% | 20/ 3.64% | 32/ 5.82% |
| A319 | 23/ 4.18% | 20/ 3.64% | 32/ 5.82% | 34/ 6.18% | 35/ 6.36% |
| A321neo | 0/ 0.00% | 16/ 2.91% | 15/ 2.73% | 12/ 2.18% | 0/ 0.00% |
| B737-8 | 141/ 25.64% | 136/ 24.73% | 137/ 24.91% | 139/ 25.27% | 134/ 24.36% |
| Total | 550/ 100.00% | 550/ 100.00% | 550/ 100.00% | 550/ 100.00% | 550/ 100.00% |

**Table 9:** Optimized Solutions across CASM Scenarios — Aircraft Count and Percentage by Type

| | CASM 1 | CASM 2 | CASM 3 | CASM 4 | CASM 5 |
|---|---|---|---|---|---|
| AIRCRAFT | Number/ % | Number/ % | Number/ % | Number/ % | Number/ % |
| A320 | 15/ 15.46% | 15/ 15.46% | 15/ 15.46% | 13/ 13.40% | 15/ 15.46% |
| A321 | 57/ 58.76% | 53/ 54.64% | 51/ 52.58% | 52/ 53.61% | 45/ 46.39% |
| A350 | 0/ 0.00% | 0/ 0.00% | 0/ 0.00% | 0/ 0.00% | 0/ 0.00% |
| B787-9 | 0/ 0.00% | 0/ 0.00% | 0/ 0.00% | 0/ 0.00% | 0/ 0.00% |
| B787-10 | 0/ 0.00% | 5/ 5.15% | 5/ 5.15% | 3/ 3.09% | 6/ 6.19% |
| ATR72 | 0/ 0.00% | 0/ 0.00% | 0/ 0.00% | 0/ 0.00% | 0/ 0.00% |
| E190 | 1/ 1.03% | 0/ 0.00% | 2/ 2.06% | 5/ 5.15% | 7/ 7.22% |
| A319 | 5/ 5.15% | 5/ 5.15% | 5/ 5.15% | 5/ 5.15% | 5/ 5.15% |
| A321neo | 0/ 0.00% | 4/ 4.12% | 3/ 3.09% | 5/ 5.15% | 0/ 0.00% |
| B737-8 | 19/ 19.59% | 19/ 19.59% | 19/ 19.59% | 19/ 19.59% | 19/ 19.59% |
| **Total** | **97/ 100.00%** | **97/ 100.00%** | **97/ 100.00%** | **97/ 100.00%** | **97/ 100.00%** |

According to Table 9's fleet count distribution, the A321 holds the largest share (46.39-58.76%), while the A320 is fixed at 15.46%, with the exception of a reduction in CASM 4, consistent with its slightly smaller seat count and lower CASM in early scenarios. The B737-8 maintained a fixed allocation of 19 units (19.59%) across all scenarios, a stable deployment independent of CASM variations. The B787-10 was introduced in CASM 2 at 5.15% share, declining to 3.09% in CASM 4 before rising to 6.19% in CASM 5, indicating responsive adjustments to long-haul with great demand. Such decline and increase were likely due to A321, which rise and decrease parallelly, ability to make up the spill cost. The E190, with a higher CASM (0.1098-0.2404) but smaller capacity, grew from 1.03% to 7.22% by CASM 5, aligning with short-haul, low-demand flights of the network. The A319 fleet remained constant, while the A321neo was used in CASM 2,3,4 yet being phased out in CASM 1,5, reflecting its low CASM ratio compared to others fleet in those used scenarios. The absence of A350, B787-9, and ATR72 aligns with their relatively higher CASM-to-RASM ratio and less suitable role for the modeled flight network. The continued absence of A350, B787-9, and ATR72 further confirms the structural characteristics of the optimized solution. Widebody aircraft such as the A350 and B787-9 are economically inefficient for the modeled domestic network due to their large seating capacity and higher operational cost while the ATR72 becomes dominated by more flexible aircraft such as the E190 and A319, which provide similar capacity levels but better cost efficiency under the assumed CASM scenarios.

Table 10 illustrates the cost distribution by aircraft type. The A321 is the dominant cost contributor (44.49-53.92%), due to its high compatibility with the network, causing high utilization. The B737-8 followed with 21.02-24.62% of total costs. The A320's share ranged between 15.45-20.30%, with absolute costs rising alongside CASM from scenario 3 onwards. The B787-10's cost share (2.61-4.37%) remained moderate despite high seat capacity, accommodating the need for long-haul flights in flight network with limited frequencies due to the network nature. The E190's cost share rose sharply to 6.18% in CASM 5, such increased deployment though relatively high CASM per seat might because low discrepancy in aircraft's seat capacity and demand. The A319 maintained ~4-5% cost share, while the A321neo peaked at 3.23% in CASM 3 before being removed from service from then. The absence of A350, B787-9, and ATR72 costs underscores their exclusion from the optimized solution, driven by their less favorable CASM positioning relative to RASM under the assumed demand conditions.

**Table 10:** Optimized Solutions across CASM Scenarios — Aircraft Cost and Percentage by Type

| | CASM 1 | CASM 2 | CASM 3 | CASM 4 | CASM 5 |
|---|---|---|---|---|---|
| AIRCRAFT | Cost/ % | Cost/ % | Cost/ % | Cost/ % | Cost/ % |
| A320 | 708,378/ 16.54% | 691,251/ 20.30% | 854,887/ 18.31% | 932,744/ 15.45% | 1,333,640/ 17.96% |
| A321 | 2,310,083/ 53.92% | 1,514,931/ 44.49% | 2,150,616/ 46.07% | 2,901,503/ 48.05% | 3,463,762/ 46.65% |
| A350 | 0/ 0.00% | 0/ 0.00% | 0/ 0.00% | 0/ 0.00% | 0/ 0.00% |
| B787-9 | 0/ 0.00% | 0/ 0.00% | 0/ 0.00% | 0/ 0.00% | 0/ 0.00% |
| B787-10 | 0/ 0.00% | 148,929/ 4.37% | 121,755/ 2.61% | 187,004/ 3.10% | 234,781/ 3.16% |
| ATR72 | 0/ 0.00% | 0/ 0.00% | 0/ 0.00% | 0/ 0.00% | 0/ 0.00% |
| E190 | 18,465/ 0.43% | 0/ 0.00% | 48,967/ 1.05% | 197,944/ 3.28% | 458,736/ 6.18% |
| A319 | 192,344/ 4.49% | 143,992/ 4.23% | 229,426/ 4.91% | 314,929/ 5.22% | 373,688/ 5.03% |
| A321neo | 0/ 0.00% | 97,663/ 2.87% | 150,848/ 3.23% | 160,463/ 2.66% | 0/ 0.00% |
| B737-8 | 1,054,617/ 24.62% | 808,722/ 23.75% | 1,111,546/ 23.81% | 1,344,039/ 22.26% | 1,560,913/ 21.02% |
| Total | 4,283,887/ 100.00% | 3,405,486/ 100.00% | 4,668,046/ 100.00% | 6,038,626/ 100.00% | 7,425,520/ 100.00% |

## 6. Conclusion

This paper presented a Genetic Algorithm (GA)-based framework for optimizing the aircraft fleet assignment problem under operational constraints. By integrating a Greedy Chain Assignment and repair mechanism, the proposed approach ensures feasible allocations that respect airport balance and fleet-size limitations while minimizing total operating and spill costs. Compared to traditional ILP, which suffers from scalability limitations, and earlier GA or ACO-based methods that often violate constraints, the proposed hybrid scheme achieves near-optimal results efficiently. Numerical evaluations on small- and large-scale test cases confirm the algorithm's scalability, stability, and close alignment with global optimal benchmarks, maintaining error margins below 0.5%. The results demonstrate the method's capability to produce cost-

effective and operationally consistent schedules. Future research may extend the proposed framework to incorporate multi-objective optimization, where additional performance criteria such as passenger service level, delay robustness, or environmental impact are considered alongside operating cost. Such an extension could allow airlines to explore trade-offs between economic efficiency and operational reliability. Furthermore, integrating schedule recovery or real-time disruption management within the proposed framework could further enhance its applicability in dynamic airline operations.

## References


Abara, J. (1989) 'Applying integer linear programming to the fleet assignment problem', Interfaces, 19(4), pp. 20-28. Available at: https://doi.org/10.1287/inte.19.4.20.

Chatziaslan, L. (2006) 'Review of Airline Operations and Scheduling by M. Bazargan', International Journal of Operations & Production Management, 26(6), pp. 689-689. Available at: https://doi.org/10.1108/01443570610667000.

Eltoukhy, A.E.E., Chan, F.T.S. and Chung, S.H. (2017) 'Airline schedule planning: a review and future directions', Industrial Management & Data Systems, 117(6), pp. 1201-1243. Available at: https://doi.org/10.1108/IMDS-09-2016-0358.

Evler, J., Lindner, M., Fricke, H. and Schultz, M. (2022) 'Integration of turnaround and aircraft recovery to mitigate delay propagation in airline networks', Computers & Operations Research, 138, 105602. Available at: https://doi.org/10.1016/j.cor.2021.105602.

Hane, C.A., Barnhart, C., Johnson, E.L., Marsten, R.E., Nemhauser, G.L. and Sigismondi, G. (1995) 'The fleet assignment problem: solving a large-scale integer program', Mathematical Programming, 70(1-3), pp. 211-232. Available at: https://doi.org/10.1007/BF01585938.

Huang, C.C., Hsu, C.C. and Collar, E. (2021). An Evaluation of the Operational Performance and Profitability of the U.S. Airlines. International Journal of Global Business and Competitiveness, Available at: https://doi.org/10.1007/s42943-021-00031-x.

Jamili, A. (2017) 'A robust mathematical model and heuristic algorithms for integrated aircraft routing and scheduling, with consideration of fleet assignment problem', Journal of Air Transport Management, 58, pp. 21-30. Available at: https://doi.org/10.1016/j.jairtraman.2016.08.008.

Li, Y. and Tan, N. (2013) 'Study on fleet assignment problem model and algorithm', Mathematical Problems in Engineering, 2013, pp. 1-5. Available at: https://doi.org/10.1155/2013/581586.

Okafor, E.G., Ubadike, O.C., Anene, N.H., Uhuegho, K.O. and Soladoye, M.A. (2019) 'Study of fleet assignment problem using a hybrid technique based on Monte Carlo simulation and genetic algorithm', Nigerian Journal of Technology, 38(3), p. 756. Available at: https://doi.org/10.4314/njt.v38i3.30.

Özdemir, Y., Başlıgil, H. and Nalbant, K.G. (2012) 'Optimization of fleet assignment: a case study in Turkey', An International Journal of Optimization and Control: Theories & Applications (IJOCTA), 2(1), pp. 59-71. Available at: https://doi.org/10.11121/ijocta.01.2012.0050.

Rashid Anzoom and Ahsan, M. (2018) 'Optimal fleet assignment using ant colony algorithm', in Proceedings of the 2018 International Conference on Production and Operations Management Society (POMS), pp. 1-6. Available at: https://doi.org/10.1109/POMS.2018.8629468.

Renegar, J. (1988) 'A polynomial-time algorithm, based on Newton's method, for linear programming', Mathematical Programming, 40-40(1-3), pp. 59-93. Available at: https://doi.org/10.1007/bf01580724.

Sun, X. et al. (2024) 'Airline competition: A comprehensive review of recent research', Journal of the Air Transport Research Society, 2(100013), pp. 1-17. Available at: https://doi.org/10.1016/j.jatrs.2024.100013.

Sherali, H.D., Bish, E.K. and Zhu, X. (2006) 'Airline fleet assignment concepts, models, and algorithms', European Journal of Operational Research, 172(1), pp. 1-30. Available at: https://doi.org/10.1016/j.ejor.2005.01.056.

V. Rao Anil (2009) 'A survey of numerical methods for optimal control', Advances in the Astronautical Sciences, 135, pp. 497-528.

Vietnam Airlines (2019) Worldwide timetable and aircraft seat map. Available at: https://www.vietnamairlines.com/~/media/FilesDownload/Plan-and-Book/Timetable/20190330-20191028/toan-mang-29mar19-EN.pdf